

Nonanalog $^{40,44}\text{Ca}(\pi^+, \pi^-)^{40,44}\text{Ti}(\text{g.s.})$ reactions at low energy

J. D. Silk,* M. Burlein,* H. T. Fortune, E. Insko, M. Kagarlis,[†] P. H. Kutt, J. M. O'Donnell,[‡] and J. D. Zumbro[§]
Department of Physics, University of Pennsylvania, Philadelphia, Pennsylvania 19104

J. A. Faucett[§], R. Garnett[§], and M.W. Rawool-Sullivan[§]
Department of Physics, New Mexico State University, Las Cruces, New Mexico 88003

C. L. Morris
Los Alamos National Laboratory, Los Alamos, New Mexico 87545

S. Saini
Oak Ridge National Laboratory, Oak Ridge, Tennessee 37831
 (Received 24 August 1994)

We present results of measurements of the forward-angle cross sections for pion double charge exchange on $^{40,44}\text{Ca}$ to the nonanalog ground states of $^{40,44}\text{Ti}$ at incident pion energies from 35 to 80 MeV. The data indicate that a substantial contribution to these cross sections arises from core polarization and/or cross-shell transitions.

PACS number(s): 25.80.Gn, 27.40.+z

The observation of a large cross section and a forward peaked angular distribution for pion double charge exchange (DCX) to the double isobaric analog state (DIAS) in the reaction $^{14}\text{C}(\pi^+, \pi^-)^{14}\text{O}(\text{g.s.})$ at 50 MeV was unexpected [1,2]. It had been thought that the destructive interference between the s and p partial wave amplitudes in pion-nucleon single charge exchange would result in a small cross section with a flat angular distribution. An excitation function and angular distribution at low energy for the reaction $^{12}\text{C}(\pi^+, \pi^-)^{12}\text{O}$ showed that the features seen in the analog transition persist in the nonanalog case [3]. A later experiment at low energy on calcium isotopes [4,5] demonstrated gross violation of the scaling of DIAS transitions with the number of pairs of excess neutrons, $\sigma \propto \frac{1}{2}(N-Z)(N-Z-1)$, which holds at higher energy [6]. Other results of DIAS studies at these low energies have demonstrated that DIAS cross sections are approximately equal on all nuclei and rapidly energy dependent. The nonanalog ^{12}O cross section is significantly smaller ($\sim \frac{1}{5}$) than the analog $^{14}\text{O}(\text{g.s.})$, but still quite large. These results have intensified interest in the nuclear structure aspects of DCX. In particular, since the DCX operator is in the simplest case a two-nucleon operator, and since we are primarily concerned with transitions to the ground state and to the DIAS, it suffices (in the case of even-even nuclei) to consider a scalar two-

nucleon operator [7,8]. For this reason it has been possible to reapply to this problem the well-understood technology which was first developed to explain the properties of nuclear ground states [9].

Following Ref. [8], if we consider 0^+ , $\nu \equiv$ seniority = 0 states of pure configurations in a single active shell, the DCX amplitude at a given angle and energy is shown to be a linear combination of a monopole amplitude and a multipole one, denoted A and B , respectively. The coefficients of these amplitudes are known functions of the neutron and proton numbers of the target and the isospins of the initial and final states. So if one knows $|A|$ and $|B|$ and their relative phase at some angle and energy, it is then easy to write down the cross sections for all the g.s. and DIAS transitions (subject to the restrictions specified above) for all the nuclei in the specified shell at that angle and energy. The coefficients of A and B are such that B alone contributes to nonanalog transitions, and the DIAS transitions scale with the number of neutron pairs only if $B = 0$.

So far the seniority model has had reasonable success in explaining several of the features seen in the data. We note two exceptions. First, this two-amplitude model has trouble fitting DCX data for the $f_{7/2}$ shell nuclei at high energy (292 MeV [10,11] and above [12]). One can greatly improve the fits by excluding either the nonanalog ground-state transitions (whose cross sections are very small) or the ^{42}Ca DIAS point (and thus allow $|B| \ll |A|$). Second, the dynamical calculations based on the model agree only qualitatively with the data, even when the calculations are corrected for the fact that the states contain nonzero seniority components.

We have measured forward-angle differential cross sections for the DCX transitions from ^{40}Ca and ^{44}Ca to the nonanalog ground states of ^{40}Ti and ^{44}Ti . We consider whether the discrepancies noted above can arise because of the presence of amplitudes not included in the

*Present address: Institute for Defense Analysis, 1801 N. Beauregard St., Alexandria, VA 22311.

[†]Present address: Niels Bohr Institute, Copenhagen, Denmark.

[‡]Present address: Los Alamos National Laboratory, Los Alamos, NM 87545.

[§]Present address: Los Alamos National Laboratory, Los Alamos, NM 87545.

TABLE I. Cross sections for $^{40,44}\text{Ca}(\pi^+, \pi^-)^{40,44}\text{Ti}$ (g.s.)

^{40}Ca			^{44}Ca		
T_π (MeV)	θ (deg)	$d\sigma/d\Omega$ ($\mu\text{b}/\text{sr}$)	T_π (MeV)	θ (deg)	$d\sigma/d\Omega$ ($\mu\text{b}/\text{sr}$)
49.09	30	0.44 ± 0.16	31.99	30	0.92 ± 0.30
	50	0.41 ± 0.13			
64.19	30	0.60 ± 0.16	47.54	30	1.4 ± 0.2
			62.83	30	0.20 ± 0.14
79.26	30	0.38 ± 0.13	78.01	30	0.18 ± 0.11

seniority-model calculations. These are the first measurements, at these low incident pion energies, of the g.s. transition on ^{40}Ca . Limited g.s. data exist for $^{44,48}\text{Ca}$ [13]. Of course, the simple seniority model mentioned above does not apply to ^{40}Ca , because the dominant transitions are expected to be of cross-shell character, i.e. [for (π^+, π^-)], $\nu(sd)^2 \rightarrow \pi(fp)^2$. Other contributions can arise from core polarization of the ^{40}Ca (g.s.), viz., $\pi(sd)^{-2} \rightarrow \nu(sd)^{-2}$ or $\nu(fp)^2 \rightarrow \pi(fp)^2$. These are of in-shell type, but by isospin selection rules, their relative phase should make them destructive. In $^{44,48}\text{Ca}$ on the other hand, in-shell transitions of the type $\nu(f_{7/2})^2 \rightarrow \pi(f_{7/2})^2$ are allowed, and are expected to dominate.

The experiment was performed at the low-energy pion channel (LEP) of the Clinton P. Anderson Meson Physics Facility (LAMPF), using the Clamshell magnetic spectrometer. Tracking information is obtained from a set of four drift chambers. Timing and differential energy loss signals are provided by thin plastic scintillators S1, S2, and S3. These are followed by four 1 in. thicknesses of scintillator, S4 – S7, so that more complete differential energy loss data may be obtained.

For the pion energies of interest in this experiment nearly all the negative outgoing pions are stopped in the scintillator stack, whereas the electrons pass through all the scintillators with small energy loss. A negative pion usually produces “stars” at the end of its trajectory, and so it is desirable to identify the pions using energy loss in the lower scintillators (S2 – S5, depending on pion energy). However, the pion energy loss peaks are overwhelmed by the Landau tails of the electron peaks in these detectors; the time of flight peak is swamped as well. Our first step therefore is to reduce the background of electrons using a tight *veto* cut on the *electron* energy loss peak in the upper detectors, S6 and S7. The electrons are thereby suppressed by a factor of roughly 20 with negligible loss of pion counts. The pion and muon peaks in the time of flight and differential energy loss histograms are now clearly visible, and the final cuts are easily made. We emphasize that pion identification is made without using energy loss measured near the ends of the pion trajectories. We thereby avoid the problem of stars in the stopping detector.

Once the pions are identified, the drift chamber efficiency can be calculated. It was found to be essentially 100%, and so no correction has been applied. We believe that our identification algorithm is also close to 100% efficient. Corrections have been made for acceptance and

in-flight decay of scattered pions, but since we normalize our cross sections by measuring known elastic scattering cross sections, these corrections (typically within 20%) nearly cancel in the ratio.

Ground-state DCX cross sections were measured at a laboratory angle of 30° and three incident pion energies, viz., 50, 65, and 80 MeV, for targets of ^{40}Ca and ^{44}Ca . An additional measurement was made at 35 MeV and 30° for ^{44}Ca , and at 50 MeV and 50° for ^{40}Ca . The ^{40}Ca target consisted of six sheets of natural calcium metal (98.94% ^{40}Ca), 0.597 g/cm² in total areal density. The ^{44}Ca target was a solid block of $^{44}\text{CaCO}_3$ (enriched at 98.4% in ^{44}Ca) powder held together with a plastic binder. The total area density was 1.5 g/cm², of which 0.99 g/cm² was CaCO_3 . Hence, the ^{44}Ca areal density was 0.414 g/cm². Relative cross sections were obtained by normalizing to the current in a toroid surrounding the primary proton beam. Absolute cross sections were obtained by measuring, in the same manner, elastic scattering of π^+ from ^{12}C at each T_π and comparing with known values of these cross sections. For ^{44}Ca , whose Q value is near zero, the target angle was set at one-half the scattering angle. For ^{40}Ca , with a large negative Q value, we used $\theta_{\text{tgt}} = \theta_{\text{scat}}$, in order to minimize energy loss of outgoing pions. Thus, cross sections in Table I are listed for T_π^A (center of target) = T_π (channel) – $\Delta E_A(T_\pi)/2 \cos \theta_{\text{tgt}}$.

The resulting differential cross sections are given in Ta-

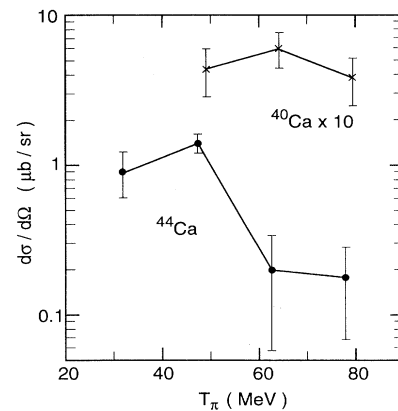


FIG. 1. Cross sections at 30° from the present work for double charge exchange on ^{44}Ca (solid circles) and ^{40}Ca (crosses) leading to ground states of ^{44}Ti and ^{40}Ti , respectively.

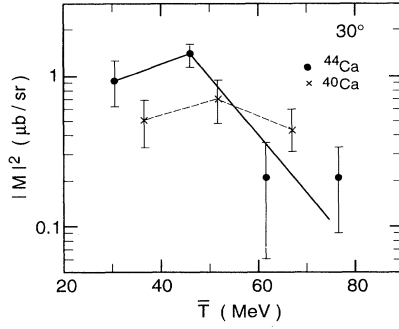


FIG. 2. Momentum weighted cross sections vs mean kinetic energy. Ordinate is $|M|^2 \equiv (k_i/k_f)d\sigma/d\Omega$, where k 's are momenta; abscissa is $\bar{T} \equiv (T_i + T_f)/2 = T_i + Q/2$.

ble I and are plotted in Fig. 1. Three aspects of the data are noteworthy. First, the cross section for the double closed shell ^{40}Ca target is not small compared to that for the ^{44}Ca target. Second, the ^{44}Ca excitation function falls sharply at the higher energies. Third, both excitation functions seem to peak in the energy range measured in this experiment. In order to remove the kinematic effects which arise from the different (nuclear) Q values (-2.9 MeV for ^{44}Ca , -24.8 MeV for ^{40}Ca), we replot the low-energy data in Fig. 2 in the form

$$|M(\bar{T})|^2 \equiv \frac{k_i}{k_f} \frac{d\sigma}{d\Omega}(T_i),$$

where T_i is the initial pion kinetic energy, $\bar{T} \equiv T_i + \frac{1}{2}Q$, and k_i (k_f) is the initial (final) pion momentum. The data sets bear a somewhat closer resemblance when plotted in this way, in both energy dependence and overall magnitude.

Recall that in the simplest models, the ^{44}Ca cross sections involve only $f_{7/2}$ nucleons, whereas (again in the simplest models) ^{40}Ca involves only cross-shell terms. The substantial cross section on ^{40}Ca demonstrates the importance of including cross-shell contributions, perhaps even for ^{44}Ca .

We might consider whether an amplitude of the magnitude which describes the observed $^{40}\text{Ca}(\pi^+, \pi^-)^{40}\text{Ti}(\text{g.s.})$ cross section can be combined with a calculated amplitude for $^{44}\text{Ca}(\pi^+, \pi^-)^{44}\text{Ti}(\text{g.s.})$ to yield the experimental value for the latter reaction. As just noted, there is some ambiguity because of the different Q values. Because the ^{40}Ca cross section varies fairly slowly with energy, these corrections are not critical. We assume that the kinematic conversion is as given above. The Q -corrected ^{40}Ca and ^{44}Ca cross sections are now for different values of the mean kinetic energy \bar{T} (see Table II). We fit a parabola through the ^{40}Ca data for the purposes of interpolation.

Because we have only one constraint on a single variable, it is not surprising that it is possible to find a solution. Of course, the relative normalization of the ^{40}Ca -

TABLE II. Momentum weighted cross sections as a function of mean kinetic energy.

\bar{T} (MeV) ^b	$ M ^2$ ^a (μ b/sr)	
	^{40}Ca	^{44}Ca
30.5		0.94 ± 0.31
36.7	0.51 ± 0.18	
46.1		1.37 ± 0.23
51.8	0.70 ± 0.22	
61.4		0.21 ± 0.15
66.9	0.45 ± 0.14	
76.6		0.21 ± 0.12

^a $|M|^2 \equiv (k_i/k_f) \frac{d\sigma}{d\Omega}$, where k_i and k_f are, respectively, incoming and outgoing pion momenta.

^b $\bar{T} \equiv (T_i + T_f)/2 = T_i + Q/2$, where $Q = -2.9$ and -24.8 MeV for ^{44}Ca and ^{40}Ca , respectively.

like" amplitude in ^{44}Ca is not known. However, if it contributes with the same normalization in ^{44}Ca as in ^{40}Ca , it is obvious from Fig. 2 that this amplitude is larger in ^{44}Ca than the $f_{7/2}$ one. With this normalization and a relative phase of 0° between the two, the resulting $f_{7/2}$ amplitudes for $^{44}\text{Ca}(\text{g.s.})$ are (in $\sqrt{\mu\text{b/sr}}$) 0.42 ± 0.16 , 0.34 ± 0.10 , at \bar{T} of 30.5 and 46.1 MeV, respectively. Thus, in this analysis, the $f_{7/2}$ contribution to the measured ^{44}Ca cross sections at these two energies is only $(18 \pm 14)\%$ and $(9 \pm 5)\%$. Larger error bars at the upper two energies preclude a meaningful extraction, but the $f_{7/2}$ amplitude would need to be quite small there.

Alternatively, we can take the $f_{7/2}^7$ predictions for ^{44}Ca from Ref. [8] and ask by what factor must the second (i.e., ^{40}Ca) amplitude be multiplied in order for the sum of the two amplitudes to fit the present ^{44}Ca data. The result is about $\frac{1}{2}$, with a relative phase near 0° .

If both amplitudes (the measured one for ^{40}Ca and the $f_{7/2}$ one from Ref. [8]) are allowed to be scaled, we find that the measured ^{44}Ca cross section is describable as having approximately equal contributions from the $f_{7/2}$ amplitude and the core amplitude. If the relative phase is 90° , no rescaling is necessary, while if the relative phase is 0° , each amplitude needs to be rescaled by a factor of about 0.7. Of course, a more serious microscopic treatment of these processes is desirable, one in which the in-shell ($f_{7/2} \rightarrow f_{7/2}$) and cross-shell ($sd \rightarrow fp$) transitions are treated on an equal footing.

Finally, we note that these g.s. cross sections are larger than those for ^{12}C [at the upper two energies the average value of $\sigma(^{40}\text{Ca})/\sigma(^{12}\text{C})$ is 2.22 ± 0.58], implying that nonanalog cross sections do not decrease with A of the target. This behavior is contrary to that observed at resonance energies, where σ goes a $A^{-4/3}$.

We acknowledge the continuing assistance of the Meson Physics division staff at LAMPF. This work was supported by grants from the National Science Foundation and the Department of Energy.

- [1] I. Navon, M.J. Leitch, D.A. Bryman, T. Numao, P. Schlatter, G. Azuelos, R. Poutissou, R.A. Burnham, M. Hasinoff, J.M. Poutissou, J.A. Macdonald, J.E. Spuller, C.K. Hargrove, H. Mes, M. Blecher, K. Gotow, M. Moinester, and H. Baer, *Phys. Rev. Lett.* **52**, 105 (1984).
- [2] M.J. Leitch, E. Piasezky, H.W. Baer, J.D. Bowman, R.L. Burman, B.J. Dropesky, P.A.M. Gram, F. Irom, D. Roberts, G.A. Rebka, Jr., J.N. Knudson, J.R. Comfort, V.A. Pinnick, D.H. Wright, and S.A. Wood, *Phys. Rev. Lett.* **54**, 1482 (1985).
- [3] J. A. Faucett, M.W. Rawool, K.S. Dhuga, J.D. Zumbro, R. Gilman, H.T. Fortune, C.L. Morris, and M.A. Plum, *Phys. Rev. C* **35**, 1570 (1987).
- [4] H. W. Baer, M.J. Leitch, R.L. Burman, M.D. Cooper, A.Z. Cui, B.J. Dropesky, G.C. Giesler, F. Irom, C.L. Morris, J.N. Knudson, J.R. Comfort, D.H. Wright, and R. Gilman, *Phys. Rev. C* **35**, 1425 (1987).
- [5] Z. Weinfeld, E. Piasezky, H.W. Baer, R.L. Burman, M.J. Leitch, C.L. Morris, D.H. Wright, S.H. Rokni, and J.R. Comfort, *Phys. Rev. C* **37**, 902 (1988).
- [6] M.B. Johnson, *Phys. Rev. C* **22**, 192 (1980).
- [7] N. Auerbach, W.R. Gibbs, and E. Piasezky, *Phys. Rev. Lett.* **59**, 1076 (1987); M. Bleszynski and R.J. Glauber, *Phys. Rev. C* **35**, 681 (1987).
- [8] N. Auerbach, W.R. Gibbs, Joseph N. Ginocchio, and W.B. Kaufmann, *Phys. Rev. C* **38**, 1277 (1988).
- [9] A. de Shalit and I. Talmi, *Nuclear Shell Theory* (Academic Press, New York, 1963).
- [10] R. Gilman, H.T. Fortune, J.D. Zumbro, C.M. Laymon, G.R. Bureson, J.A. Faucett, W.B. Cottingham, C.L. Morris, P.A. Seidl, C.F. Moore, L.C. Bland, R.R. Kiziah, S. Mordechai, and K.S. Dhuga, *Phys. Rev. C* **35**, 1334 (1987).
- [11] J.D. Zumbro, H.T. Fortune, M. Burlein, C.L. Morris, Z.F. Wang, R. Gilman, K.S. Dhuga, G.R. Bureson, M.W. Rawool, R.W. Garnett, M.J. Smithson, D.S. Oakley, S. Mordechai, C.F. Moore, M.A. Machuca, D.L. Watson, and N. Auerbach, *Phys. Rev. C* **36**, 1479 (1987).
- [12] A.L. Williams, J.A. McGill, C.L. Morris, G.R. Bureson, D.S. Oakley, J.A. Faucett, M. Burlein, H.T. Fortune, J.M. O'Donnell, G.P. Kahrmanis, and C.F. Moore, *Phys. Rev. C* **43**, 766 (1991); A.L. Williams, K.W. Johnson, G.P. Kahrmanis, H. Ward, C.F. Moore, J.A. McGill, C.L. Morris, G.R. Bureson, J.A. Faucett, M. Rawool-Sullivan, D.S. Oakley, M. Burlein, H.T. Fortune, E. Insko, R. Ivie, J.M. O'Donnell, and D. Smith, *ibid.* **44**, 2025 (1991).
- [13] M.J. Leitch, H.W. Baer, A. Klein, C.S. Mishra, Z. Weinfeld, E. Piasezky, Y. Ezra, R. Weiss, C. Allgower, J.R. Comfort, J. Tinsley, and D.H. Wright, *Phys. Lett. B* **294**, 157 (1992).